

COORDINATED MULTIWAVELENGTH OBSERVATIONS AND SPECTRAL VARIABILITY MODELING OF GAMMA-RAY BLAZARS

Markus Böttcher

Department of Physics and Astronomy, Ohio University, Athens, OH 45701, USA

ABSTRACT

Our recent progress on time-dependent modeling of the multiwavelength spectra and variability of blazars with leptonic and hadronic jet models is reviewed. Special emphasis is placed on X-ray spectral variability of low-frequency peaked (LBLs) and intermediate BL Lac objects (IBLs). As an example, recent observational and modeling results of an extensive multiwavelength campaign of BL Lacertae in 2000 are presented. It is demonstrated how combined spectral and variability modeling of LBLs and IBLs can significantly constrain emission models and potential variability scenarios. In the case of BL Lacertae, the variability appears to be driven primarily by fluctuations in the spectral index of the non-thermal, ultrarelativistic electron population in the jet. Such constraints allow us to refine predictions of the intrinsic GeV γ -ray emission and the dominant electron cooling mechanism in these objects.

Key words: Active galactic nuclei; blazars; BL Lacertae; jets; gamma-rays; multiwavelength observations; theory.

1. INTRODUCTION

Blazars are the most extreme class of active galaxies known to date. They have been observed in all wavelength bands — from radio through very-high energy (VHE) γ -ray frequencies. 66 blazars have been identified as sources of > 100 MeV emission detected by the EGRET telescope on board the *Compton Gamma-Ray Observatory* (CGRO; Hartman et al., 1999), and 6 blazars (Mrk 421: Punch et al. (1992); Petry et al. (1996); Mrk 501: Quinn et al. (1996); Bradbury et al. (1997); PKS 2155-314: Chadwick et al. (1999); 1ES 2344+514: Catanese et al. (1998); 1H 1426+428: Horan et al. (2002); Aharonian et al. (2002); 1ES 1959+650: Nishiyama et al. (1999); Holder et al. (2003); Aharonian et al. (2003)) have now been detected at VHE γ -rays (> 350 GeV) by ground-based air Čerenkov telescopes. Many of the EGRET-detected

γ -ray blazars appear to emit — at least temporarily — the bulk of their bolometric luminosity at γ -ray energies. Blazars exhibit variability at all wavelengths on time scales — in some cases — down to less than an hour. VLBI radio observations and monitoring often reveal one-sided kpc-scale jet structures, exhibiting apparent superluminal motion. The radio through optical emission from blazars often shows linear polarization, pointing towards a synchrotron origin.

1.1. Blazar Spectra

The broadband continuum spectra of blazars are dominated by non-thermal emission and consist of at least two clearly distinct, broad spectral components. A sequence of sub-classes of blazars can be defined through the peak frequencies and relative νF_ν peak fluxes of those components, which also appear to be correlated with the overall bolometric luminosity of the sources (Fossati et al., 1998): In the case of flat-spectrum radio quasars (FSRQs), the low-frequency (synchrotron) component extends from radio to optical/UV frequencies, with a peak frequency generally in the mm or IR band; the high-frequency component extends from X-rays through GeV γ -ray energies, with a νF_ν peak frequency corresponding to ~ 10 MeV — 1 GeV. No FSRQ has so far been detected by ground-based air Čerenkov telescope facilities at energies > 100 GeV, although in flaring states the γ -ray νF_ν peak flux of FSRQs dominates over the low-frequency emission by up to ~ 1 order of magnitude. In the case of high-frequency peaked BL Lac objects (HBLs), the low-frequency component often extends far into the X-rays, with peak frequencies ranging from the UV/soft X-ray to the hard X-ray regime (Pian et al., 1998), depending on the source and its state of activity; the high-energy component of HBLs extends from hard X-rays far into the VHE γ -ray regime. All blazars detected at VHE γ -ray energies to date are HBLs. In spite of extending to extremely high photon energies, the νF_ν peak flux of the γ -ray component of HBLs is generally at most comparable to the spectral output in the low-frequency component. In terms of their overall bolometric luminosity, FSRQs appear to be

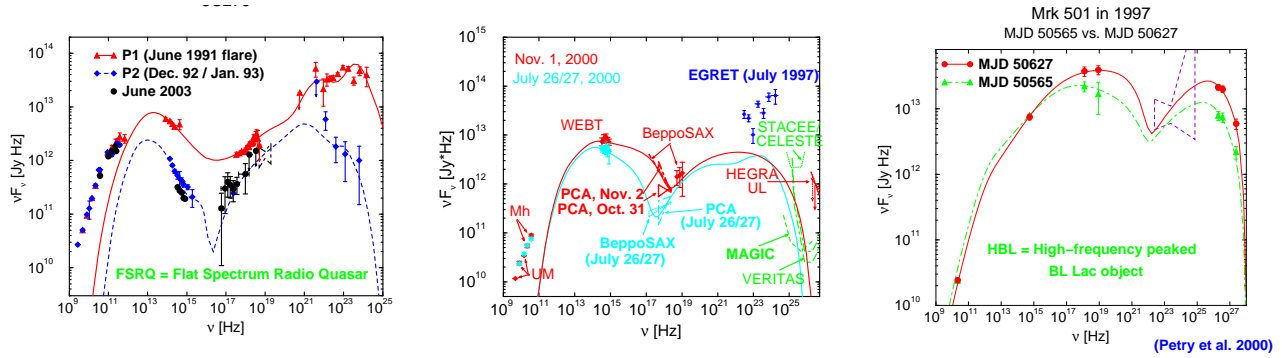


Figure 1. Broadband spectra of the FSRQ 3C 279 (left panel; Hartman et al., 2001a; Collmar et al., 2004), the LBL BL Lacertae (middle panel; Böttcher et al., 2003), and the HBL Mrk 501 (Petry et al., 2000). For each object, two simultaneous SEDs at two different epochs are shown, illustrating the range of long-term spectral variability seen in these objects. For 3C 279, the results of recent multiwavelength observations in 2003, including *INTEGRAL* (Collmar et al., 2004) are also shown.

several orders of magnitude more powerful sources than HBLs.

Apparently intermediate between the FSRQs and the HBLs are the low-frequency peaked BL Lac objects (LBLs). The peak of their low-frequency component is typically located at IR or optical wavelengths, their high-frequency component peaks typically at \sim several GeV, and the γ -ray output is of the order of or slightly higher than the level of the low-frequency emission. Fig. 1 shows a compilation of broadband spectra of a typical FSRQ (3C279), an LBL (BL Lacertae), and an HBL (Mrk 501), respectively. Each panel shows the respective object at two or three different observing epochs, in two different activity states.

1.2. Blazar Variability

Fig. 1 already illustrates that in particular the high-energy emission from blazars can easily vary by more than an order of magnitude between different observing epochs. However, variability has been observed on much shorter time scales, in some extreme cases less than an hour (Gaidos et al., 1996). Fig. 2 shows examples of light curves of the LBL BL Lacertae, taken during a broadband observing campaign carried out in the second half of 2000 (Böttcher et al., 2003; Villata et al., 2002). While the radio emission of blazars is generally variable on time scales of weeks – months (Fig. 2a), the optical light curve shows significant variability on time scales down to \sim 1.5 hr (Fig. 2b).

Often, both the optical and X-ray emission show characteristic hardness-intensity correlations. Fig. 3 illustrates this for BL Lacertae in 2000. Some HBLs (e.g., Mrk 421 and PKS 2155-304) have been observed to exhibit characteristic, clockwise loop structures (“spectral hysteresis”; Takahashi et al., 1996; Kataoka et al., 2000), which can be interpreted as the synchrotron radiation signature of gradual injection and/or acceleration of ul-

trarelativistic electrons into the emitting region, and subsequent radiative cooling (Kirk et al., 1998; Georganopoulos & Marscher, 1998; Kataoka et al., 2000; Kusunose et al., 2000; Li & Kusunose, 2000).

In LBLs, the soft X-ray emission is also sometimes dominated by the high-energy end of the synchrotron emission component, so similar spectral hysteresis phenomena should in principle be observable. However, those objects are generally much fainter at X-ray energies than their high-frequency peaked counterparts, making the extraction of time-dependent spectral information an observationally very challenging task. Fig. 3 clearly illustrates that the *BeppoSAX* observations of BL Lacertae in 2000 revealed evidence for spectral variability, but lacked the sensitivity to clearly establish or rule out spectral hysteresis. Such a measurement might require the new generation of X-ray telescopes such as *Chandra* or *XMM-Newton*.

2. OVERVIEW OF LEPTONIC JET MODELS OF BLAZARS

The high apparent bolometric luminosity combined with the short variability time scales and the apparent superluminal motions of individual jet components observed in many blazars, provide compelling evidence that the nonthermal continuum is produced in emission regions of a typical size scale of \sim a few light days or less, moving relativistically along a jet structure which is directed at a small angle with respect to our line of sight. The jets are most likely powered by accretion of circumnuclear matter onto a supermassive black hole of $10^8 M_{\odot} \lesssim M_{\text{BH}} \lesssim 10^{10} M_{\odot}$. The emission regions are characterized by the presence of an ultrarelativistic population of nonthermal electrons. Several scenarios have been proposed concerning the acceleration of such ultrarelativistic electrons, including impulsive injection near the base of the jet (Dermer & Schlickeiser, 1993; Böttcher et al., 1997), individual shock waves propagating along

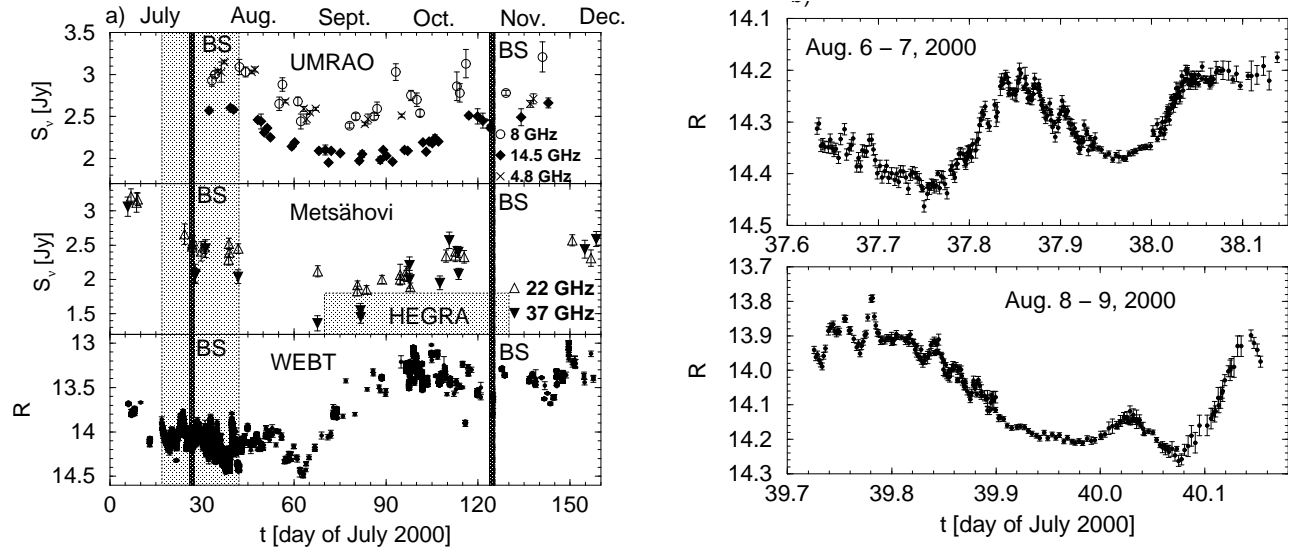


Figure 2. Radio and optical light curves of the LBL BL Lacertae during the multiwavelength campaign of 2000. The dark-shaded areas in panel a) indicate the time segments of BeppoSAX observations.

the jet Marscher & Gear (1985), relativistic particle acceleration at shear layers between a fast-moving inner jet and a slower moving outer jet (e.g., Stawarz & Ostrowski, 2003) or internal shocks from the collisions of multiple shells of material ejected into the jet structure (Spada et al., 2001). Because of the difficulty of constraining the acceleration mechanism and the composition and spectral characteristics of the injected particle distribution (see, e.g., Sikora & Madejski, 2000; Ostrowski & Bednarz, 2002; Stawarz & Ostrowski, 2003), the time profile of injection and injected particle spectra of ultrarelativistic electrons are generally treated as free parameters in blazar modeling.

The nonthermal electrons are emitting synchrotron radiation, which is responsible for the low-frequency emission from radio to UV or even X-ray frequencies. Higher-frequency (X-ray and γ -ray) emission is produced via Compton scattering processes. Possible target photon fields for Compton scattering are the synchrotron photons produced within the jet (the SSC process; Marscher & Gear, 1985; Maraschi et al., 1992; Bloom & Marscher, 1996), or external photons (the EC process). Sources of external seed photons include the UV – soft X-ray emission from the disk — either entering the jet directly (Dermer et al., 1992; Dermer & Schlickeiser, 1993) or after reprocessing in the broad line region (BLR) or other circumnuclear material (Sikora et al., 1994; Blandford & Levinson, 1995; Dermer et al., 1997) —, jet synchrotron radiation reflected at the BLR (Ghisellini & Madau, 1996; Bednarek, 1998; Böttcher & Dermer, 1998), or the infrared emission from circumnuclear dust (Blażejowski et al., 2000; Arbeiter et al., 2002). In the context of jet model invoking a significant deceleration of the outflow along the jet, an important source of soft photons might also be provided by the synchrotron photons from slower portions of the jet further downstream

(Georganopoulos & Kazanas, 2003).

In addition to these fundamental radiation processes, $\gamma\gamma$ absorption and pair production as well as synchrotron self absorption have to be taken into account in order to build a self-consistent blazar radiation model. Synchrotron self absorption is the reason why some of the spectral fits shown in Fig. 1 do not reproduce the radio spectra of the respective sources: The emission regions are optically thick at radio frequencies during the early stages of propagation of the emission regions through the jet, where the non-thermal electron population is sufficiently energetic to produce ample high-energy radiation.

As the emission region is moving relativistically outward, the nonthermal electron population will evolve according to

$$\frac{\partial n_e(\gamma, t)}{\partial t} = -\frac{\partial}{\partial \gamma} \left(\left[\frac{d\gamma}{dt} \right]_{\text{acc/loss,cont.}} n_e[\gamma, t] \right) + q_e(\gamma, t) - p_e(\gamma, t) + Q_e(\gamma, t) - \frac{n_e(\epsilon, t)}{t_{e,\text{esc}}}, \quad (1)$$

where $(d\gamma/dt)_{\text{acc/loss,cont.}}$ denotes the continuous energy losses due to radiative and adiabatic cooling and energy gain due to acceleration processes, p_e and q_e are the terms describing the population and depopulation of a given electron energy interval due to non-continuous energy loss processes (such as Compton scattering, in particular in the Klein-Nishina regime), Q_e describes the electron injection function, and $t_{e,\text{esc}}$ is the escape time scale of nonthermal electrons. The evolution of the photon population in the emission region has to be solved simultaneously with the electron distribution, and is determined through

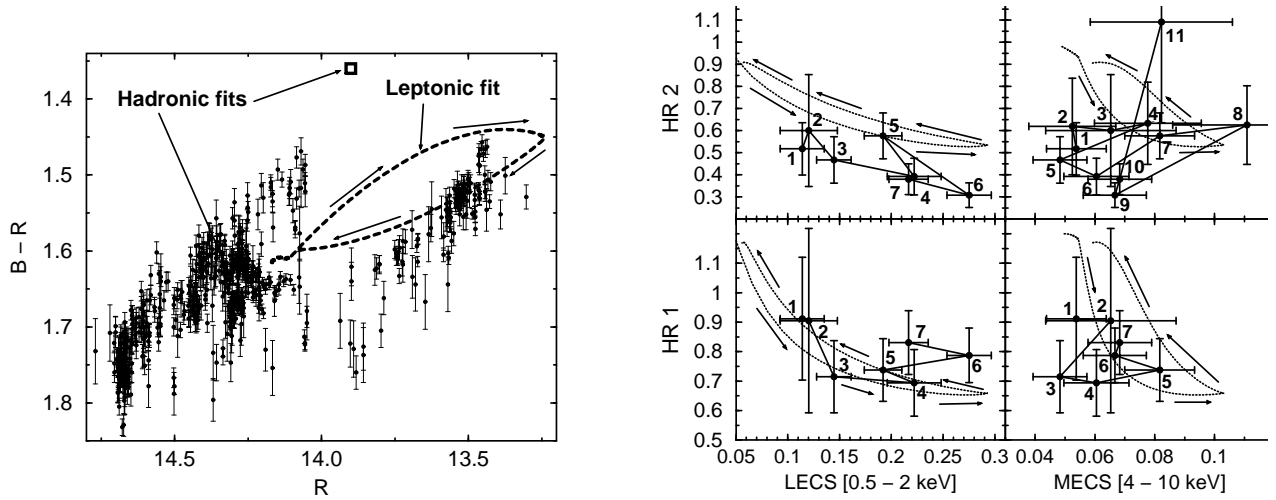


Figure 3. Left panel (a): Optical color-magnitude relation observed during the multiwavelength campaign on BL Lacertae in 2000 (Villata et al., 2002; Böttcher et al., 2003; Böttcher & Reimer, 2004). Right panel (b): X-ray hardness-intensity diagram extracted from BeppoSAX observations. The curves indicate the spectral variability patterns from the best-fit leptonic model of Böttcher & Reimer (2004).

$$\frac{\partial n_{\text{ph}}(\epsilon, t)}{\partial t} = \dot{n}_{\text{ph,em}}(\epsilon, t) - \dot{n}_{\text{ph,abs}}(\epsilon, t) + q_{\text{ph}}(\epsilon, t) - p_{\text{ph}}(\epsilon, t) - \frac{n_{\text{ph}}(\epsilon, t)}{t_{\text{ph,esc}}} \quad (2)$$

where now $\dot{n}_{\text{ph,em}}$ and $\dot{n}_{\text{ph,abs}}$ describe the fundamental emission and absorption processes, q_{ph} and p_{ph} describe the scattering rates into and out of a given photon energy bin, and $t_{\text{ph,esc}}$ is the photon escape time scale.

2.1. Leptonic-Jet Spectral Modeling Results for Different Blazar Classes

Various versions of the generic leptonic jet model described in the previous section have been used very successfully to model simultaneous broadband spectra of several FSRQs, LBLs, and HBLs. As more detailed spectral information has become available, the results of such broadband spectral modeling have now converged towards a rather consistent picture (Ghisellini et al., 1998; Kubo et al., 1998). The spectral sequence HBLs \rightarrow LBLs \rightarrow FSRQs appears to be related to an increasing contribution of the external Comptonization mechanism to the γ -ray spectrum. While most FSRQs are successfully modelled with external Comptonization models (e.g., Dermer et al., 1997; Sambruna et al., 1997; Mukherjee et al., 1999; Hartman et al., 2001a), the broadband spectra of HBLs are consistent with pure SSC models (Mastichiadis & Kirk, 1997; Pian et al., 1998; Petry et al., 2000; Krawczynski et al., 2002). BL Lacertae, a LBL, appears to be intermediate between these two extremes, requiring an external Comptonization component to explain the EGRET spectrum (Madejski et al., 1999; Böttcher & Bloom, 2000). One generally finds that HBLs require higher

average electron energies and lower magnetic fields than LBLs and FSRQs. In most cases, the required Doppler boosting factors D seem to be comparable for all types of objects, although there have also been some results indicating an extraordinarily high value of $D \gtrsim 40$ for the HBL Mrk 501 (Krawczynski et al., 2002). Typical examples of broadband spectral fits consistent with this sequence of leptonic jet model parameters are shown in Fig. 1. The occasional finding of very high Doppler factors, in particular in some HBLs, has prompted Georganopoulos & Kazanas (2003) to propose their model of a decelerating, stratified jet in which synchrotron photons from slower regions of the jet would serve as seed photons for Compton scattering, appearing slightly blue shifted in the rest frame of the faster high-energy emission region further upstream. Such a scenario could remove the need for bulk Lorentz factors largely in excess of ~ 10 for HBLs.

2.2. Leptonic-Jet Modeling of Blazar Spectral Variability

The generic blazar model described above is inherently time-dependent and facilitates the modeling not only of the broadband SEDs, but also the detailed spectral variability of blazars. Studies of blazar spectral variability have been done in great detail for the case of pure SSC models with electron cooling dominated by synchrotron losses, e.g., by Kirk et al. (1998); Georganopoulos & Marscher (1998); Kataoka et al. (2000); Kusunose et al. (2000); Li & Kusunose (2000). In those papers, the spectral hysteresis observed in several HBLs was reproduced, significantly constraining model parameters beyond constraints obtainable from pure spectral modeling. More recently, Sikora et al. (2001) have extended these studies to an inho-

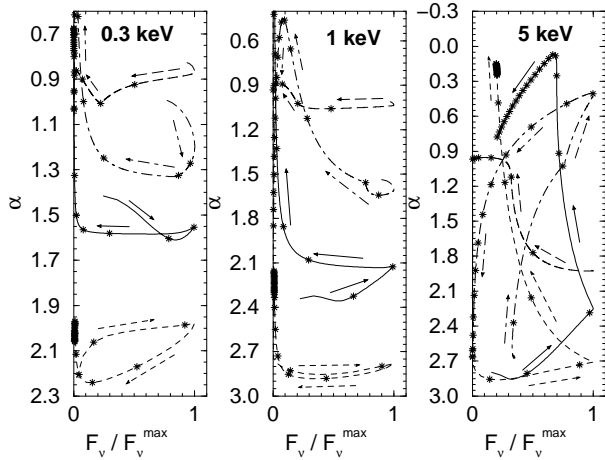


Figure 4. Comparison of the tracks in the flux – spectral-index plane for different generic jet models, from synchrotron-dominated (short-dashed) to SSC dominated (long-dashed). From Böttcher & Chiang (2002).

homogeneous jet model, also including an external Compton component, so that the model would now also be applicable to LBLs and quasars. They have applied their model to the special case of 3C 279. Based on their results, they interpreted the lack of a measurable time lag between the γ -ray and X-ray emission in that object (Hartman et al., 2001b) as evidence that X-rays and γ -rays might be produced co-spatially by electrons of similar energies. This, in turn, provides evidence for two separate emission components being dominant at X-rays and γ -rays. Most plausibly, this might indicate that the X-ray emission is dominated by SSC emission, while the γ -rays are dominated by external Compton emission.

Time-dependent, homogeneous leptonic jet models in which radiation mechanisms other than synchrotron may dominate have recently been investigated in an analytical approach by Chiang & Böttcher (2002), and with detailed numerical simulations by Böttcher & Chiang (2002). Chiang & Böttcher (2002) pointed out that a dominant contribution from SSC to the electron cooling will produce a characteristic time-averaged synchrotron spectral index of $\alpha = 3/2$ (energy spectral index), independent of the injection index of relativistic electrons in the jet. In this case, the cooling time scale of electrons radiating at a synchrotron photon energy E_{sy} is expected to scale as $\tau_{\text{cool,SSC}} \propto E_{\text{sy}}^{(q-4)/2}$, where q is the electron injection spectral index (Böttcher et al., 2003). This differs characteristically from the synchrotron or EC dominated case in which $\tau_{\text{cool,sy}} \propto E_{\text{sy}}^{-1/2}$, independent of the electron injection index q .

Detailed numerical simulations of the time-dependent emission characteristics of homogeneous jet models with parameters specifically chosen to be appropriate for low-frequency peaked and intermediate BL Lac objects have been done by

Böttcher & Chiang (2002). A key result of their study was that a dominant SSC component would leave very obvious imprints in the X-ray spectral variability of these objects, as illustrated in Fig. 4. In contrast, they found that a moderate and even slightly dominant contribution from external Compton scattering will have virtually no effect on the X-ray spectral variability patterns. This might be a consequence of the fact that the beaming pattern of external Compton emission is more strongly peaked in the forward direction than the synchrotron and SSC components (which are assumed to be isotropic in the co-moving frame of the emission region). Thus, even if the EC component is dominating the γ -ray emission at MeV – GeV energies, it may only make a moderate contribution to the electron cooling rate. The results of Böttcher & Chiang (2002) have been applied in detail to simultaneous multiwavelength observations of W Comae in 1998 (Böttcher et al., 2002) and BL Lacertae in 2000 (Böttcher & Reimer, 2004).

3. OVERVIEW OF HADRONIC BLAZAR MODELS

While leptonic models deal with a relativistic e^\pm plasma in the jet, in hadronic models the relativistic jet consists of a relativistic proton (p) and electron (e^-) component. In the following, a brief summary of the Synchrotron-Proton Blazar (SPB-) model (Mücke et al., 2003) is given, as an example of a hadronic model that takes into account all the salient features of hadronic blazar jet models in general.

Like in the leptonic model, the emission region in an AGN jet moves relativistically along the jet axis which is closely aligned with our line of sight. Relativistic protons, whose particle density n_p follows a power law spectrum $\propto \gamma_p^{-q_p}$ in the range $2 \leq \gamma_p \leq \gamma_{p,\text{max}}$, are injected instantaneously into a highly magnetized environment ($B = \text{const.}$ within the emission region), and are subject to energy losses due to proton-photon interactions (meson production and Bethe-Heitler pair production), synchrotron radiation and adiabatic expansion. The mesons produced in photonmeson interactions always decay in astrophysical environments. However, they may suffer synchrotron losses before the decay, which is taken into account in this model.

If the relativistic electrons are accelerated together with the protons at the same site, their injection spectrum shows most likely the same spectral shape $\propto \gamma_e^{-q_e}$ with $q_e = q_p$. The relativistic primary e^- radiate synchrotron photons which constitute the low-energy bump in the blazar SED, and serve as the target radiation field for proton-photon interactions and the pair-synchrotron cascade which subsequently develops. The SPB-model is designed for objects with a negligible external target photon component, and hence suitable for BL Lac objects. The cascade re-

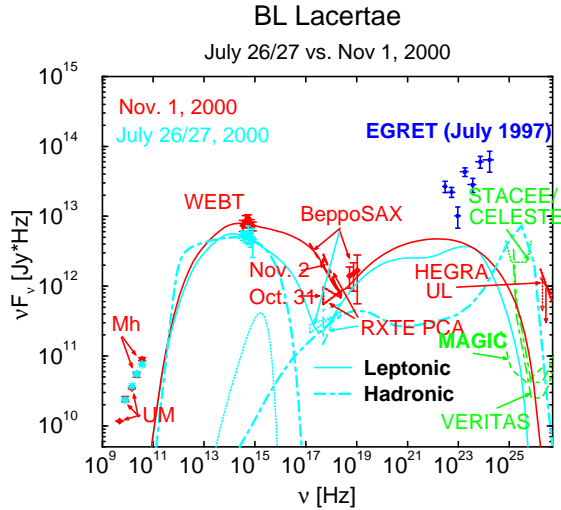


Figure 5. Best-fit time-averaged leptonic (solid curves) and hadronic (dot-dashed curves) models for BL Lacertae in 2000 (Böttcher & Reimer, 2004).

distributes the photon power to lower energies where the photons eventually escape from the emission region. The cascades can be initiated by photons from π^0 -decay (“ π^0 cascade”), electrons from the $\pi^\pm \rightarrow \mu^\pm \rightarrow e^\pm$ decay (“ π^\pm cascade”), p -synchrotron photons (“ p -synchrotron cascade”), charged μ^- , π^- and K -synchrotron photons (“ μ^\pm -synchrotron cascade”) and e^\pm from proton-photon Bethe-Heitler pair production (“Bethe-Heitler cascade”).

Because “ π^0 cascades” and “ π^\pm cascades” generate rather featureless photon spectra (Mücke & Protheroe, 2001; Mücke et al., 2003), proton and muon synchrotron radiation and their reprocessed radiation turn out to be mainly responsible for the high energy photon output in blazars. The contribution from the Bethe-Heitler cascades is mostly negligible. The low energy component is dominated by synchrotron radiation from the primary e^- , with a small contribution of synchrotron radiation from secondary electrons (produced by the p - and μ^\pm -synchrotron cascade). A detailed description of the model itself, and its implementation as a (time-independent) Monte-Carlo code, has been given in Mücke & Protheroe (2001) and Reimer et al. (2004). This code has been used, e.g., to generate the spectral fits presented in Böttcher & Reimer (2004) for BL Lacertae in 2000 (see also Fig. 5).

4. MODELING RESULTS FOR BL LACERTAE IN 2000

Both the leptonic and hadronic models described in the previous sections have been applied successfully to the data obtained during the multiwavelength observing campaign on BL Lacertae in 2000 (Böttcher et al., 2003). The best time-averaged spectral fits are shown in Figs. 1 and 5. The best-fit

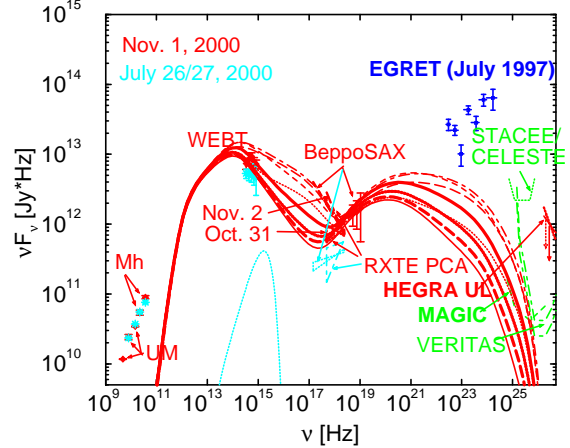


Figure 6. Time-dependent model spectra from the best-fit leptonic model for BL Lacertae in 2000 (Böttcher & Reimer, 2004). The time sequence is: thin solid \rightarrow thin dotted \rightarrow thin long-dashed \rightarrow thin dot-dashed \rightarrow thin short-dashed \rightarrow thick solid \rightarrow thick dotted \rightarrow thick long-dashed, in equi-distant time steps of $\Delta t_{\text{obs}} \approx 1 \text{ hr}$.

parameters for the leptonic and hadronic model fits differ substantially in the following ways: (a) The overall jet power required in the hadronic models is ~ 2 orders of magnitude higher than for the leptonic models ($\sim 6 \times 10^{44} \text{ ergs s}^{-1}$ vs. $\lesssim 6 \times 10^{42} \text{ ergs s}^{-1}$); (b) the magnetic fields in hadronic jet models are a factor of ~ 20 higher than for leptonic models ($B \sim 30 - 40 \text{ G}$ vs. $\sim 2 \text{ G}$), and the bulk Lorentz factor of the emission region is a factor of ~ 2 lower for the hadronic models ($\sim 7 - 9$ vs. ~ 18).

Considering the time-averaged emission of BL Lacertae in 2000, hadronic models predict a sustained level of multi-GeV – TeV emission which should be detectable with second-generation atmospheric Cherenkov telescope systems like VERITAS, HESS, or MAGIC. In contrast, our leptonic model only predicts a peak flux exceeding the anticipated nominal MAGIC sensitivity during short flares; the accumulated fluence over observing time scales of several hours might not be sufficient for a significant detection. Thus, a future VHE detection of BL Lacertae would be a strong indication for hadronic processes being at work in this object.

The detailed spectral evolution of our best-fit leptonic jet simulation is shown in Fig. 6. In order to determine the best-fit variability scenario, various generic flaring scenarios had been investigated and compared to the observed optical and X-ray spectral variability patterns (see Fig. 3). Specifically, we had investigated scenarios invoking a temporary increase in jet power, a flattening of the electron injection spectral index, an increasing high-energy cutoff γ_2 of the electron injection spectrum, and various combination of these. Other parameter fluctuations could be ruled out on the basis of general, analytical con-

siderations, without detailed simulations. We found that the observed optical and X-ray spectral variability in BL Lacertae in 2000 can be reproduced through short-term fluctuations of only the electron injection spectral index, with all other parameters remaining unchanged.

Remarkably, our time-dependent fits indicated that an injection index larger than $q \sim 2.3$, even during the peak of an individual short-term flare, is required. If the injection of ultrarelativistic electrons into the emitting volume is caused by Fermi acceleration at relativistic shocks, detailed numerical studies have shown that with fully developed turbulence in the downstream region, a unique asymptotic index of $q \sim 2.2 - 2.3$ should be expected (e.g., Achterberg et al., 2001; Gallant et al., 1999). However, recently Ostrowski & Bednarz (2002) have shown that Fermi acceleration might lead to drastically steeper injection spectra if the turbulence is not fully developed. Furthermore, depending on the orientation of the magnetic field at the shock front, an abrupt steepening of the injection spectra may result if the shock transits from a subluminal to a superluminal configuration. In this context, our leptonic fit results may indicate that such predominantly geometric effects, may be the cause of the rapid variability observed in BL Lacertae.

Our spectral-variability simulation predicted counter-clockwise spectral hysteresis at X-ray energies. Such hysteresis was not predicted in the specific SPB model fits presented in Böttcher & Reimer (2004), but could not clearly be ruled out either. Thus, sensitive spectral-hysteresis measurements of BL Lacertae could possibly serve as a test of our modeling results and a secondary diagnostic to distinguish between leptonic and hadronic models, though, by itself, it would not be sufficient as a model discriminant.

Ravasio et al. (2003) had previously noted the discrepancy between the time-averaged optical and X-ray spectra (Ravasio et al., 2003) which could not be joined smoothly by an absorbed power-law spectrum. They had considered several possibilities to explain this discrepancy, including additional particle populations, extreme Klein-Nishina effects on the electron cooling rates, and/or anomalies in the intergalactic absorption. Our successful modeling of the observed time-dependent flux and hardness values at optical and X-ray frequencies in the framework of a leptonic model effectively removes the need for such additional assumptions and indicates that the time-averaging involved in compiling the detailed broadband spectral energy distribution may be the cause of this apparent discrepancy.

ACKNOWLEDGMENTS

This work was partially supported by NASA through INTEGRAL GO Program Grants no. NAG 5-13205 and NAG 5-13684.

REFERENCES

- Achterberg, A., Gallant, Y. A., Kirk, J. G., & Guthmann, A. W., 2001, *MNRAS*, 328, 393
- Aharonian, F. A., et al., 2002, *A&A*, 384, L23
- Aharonian, F. A., et al., 2003, *A&A*, 406, L9
- Arbeiter, C., Pohl, M., & Schlickeiser, R., 2002, *A&A*, 386, 415
- Bednarek, W., *A&A*, 342, 69
- Blandford, R. D., & Levinson, A., 1995, *ApJ*, 441, 79
- Blażejowski, M., et al., 2000, *ApJ*, 545, 107
- Bloom, S. D., & Marscher, A. P., 1996, *ApJ*, 461, 657
- Böttcher, M., Mause, h., & Schlickeiser, R., 1997, *A&A*, 324, 395
- Böttcher, M., & Bloom, S. D., 2000, *AJ*, 119, 469
- Böttcher, M., & Chiang, J., 2002, *ApJ*, 581, 127
- Böttcher, M., & Dermer, C. D., 1998, *ApJ*, 501, L51
- Böttcher, M., et al., 2003, *ApJ*, 598, 847
- Böttcher, M., Mukherjee, R., & Reimer, A., 2002, *ApJ*, 581, 143
- Böttcher, M., & Reimer, A., 2004, *ApJ*, submitted
- Bradbury, S. M., 1997, *A&A*, 320, L5
- Catanese, M., et al., 1998, *ApJ*, 501, 616
- Chadwick, P. M., 1999, *ApJ*, 513, 161
- Chiang, J., & Böttcher, M., 2002, *ApJ*, 564, 92
- Collmar, W., et al., 2004, these proceedings
- Dermer, C. D., Schlickeiser, R., & Mastichiadis, A., 1992, *A&A*, 256, L27
- Dermer, C. D., & Schlickeiser, R., 1993, *ApJ*, 416, 458
- Dermer, C. D., Sturmer, S. J., & Schlickeiser, R., 1997, *ApJS*, 109, 103
- Fossati, G., 1998, *MNRAS*, 299, 433
- Gaidos, J. A., et al., 1996, *Nature*, 383, 319
- Gallant, Y. A., Achterberg, A., & Kirk, J. G., 1999, *A&AS*, 138, 549
- Georganopoulos, M., & Kazanas, D., 2003, *ApJ*, 594, L27
- Georganopoulos, M., & Marscher, A. P., 1998, *ApJ*, 506, L11
- Ghisellini, G., & Madau, P., 1996, *MNRAS*, 280, 67
- Ghisellini, G., et al., 1998, *MNRAS*, 301, 451
- Hartman, R. C., et al., 1999, *ApJS*, 123, 79
- Hartman, R. C., et al., 2001a, *ApJ*, 553, 683
- Hartman, R. C., et al., 2001b, *ApJ*, 558, 583
- Holder, J., et al., 2003, *ApJ*, 583, L9
- Horan, D., et al., 2002, *ApJ*, 571, 753
- Kataoka, J., et al., 2000, *ApJ*, 528, 243
- Kirk, J. G., Rieger, F. M., & Mastichiadis, A., *A&A*, 333, 452

- Krawczynski, H., Coppi, P. S., & Aharonian, F. A., 2002, MNRAS, 336, 721
- Kubo, H., et al., 1998, ApJ, 504, 693
- Kusunose, M., Takahara, F., & Li, H., 2000, ApJ, 536, 299
- Li, J., & Kusunose, M., 2000, ApJ, 536, 729
- Madejski, G., et al., 1999, ApJ, 521, 145
- Maraschi, L., Ghisellini, G., & Celotti, A., 1992, 397, L5
- Marscher, A. P., & Gear, W. K., 1985, ApJ, 298, 114
- Mastichiadis, A., & Kirk, J. G., 1997, A&A, 320, 19
- Mücke, A., & Protheroe, R. J., 2001, Astropart. Phys., 15, 121
- Mücke, A., Protheroe, R. J., Engel, R., Rachen, J. P., & Stanev, T., 2003, Astropart. Phys., 18, 593
- Mukherjee, R., et al., 1999, ApJ, 527, 132
- Nishiyama, T., et al., in Proc. of the 26th ICRC, 3, 370
- Ostrowski, M., & Bednarz, J., 2002, A&A, 394, 1141
- Petry, D., et al., 1996, A&A, 311, L13
- Petry, D., et al., 2000, ApJ, 536, 742
- Pian, E., 1998, ApJ, 492, L17
- Punch, M., et al., 1992, Nature, 358, 477
- Quinn, J., et al., ApJ, 456, L83
- Ravasio, M., Tagliaferri, G., Ghisellini, G., Tavacchio, F., Böttcher, M., & Sikora, M., 2003, A&A, 408, 479
- Reimer, A., Protheroe, R. J., & Donea, A.-C., 2004, A&A, in press
- Sambruna, R., et al., 1997, ApJ, 474, 639
- Sikora, M., & Madejski, G., 2000, ApJ, 534, 109
- Sikora, M., et al., 2001, ApJ, 554, 1; Erratum: ApJ, 561, 1154 (2001)
- Spada, M., MNRAS, 325, 1559
- Sikora, M., Begelman, M. C., & Rees, M. J., 1994, ApJ, 421, 153
- Stawarz, L., & Ostrowski, M., 2003, New Astron. Rev., 47, 6-7, 521
- Takahashi, T., et al., 1996, ApJ, 470, L89
- Villata, M., et al., 2002, A&A, 390, 407